Available online at www.sciencedirect.com
SCIENCE DIRECT®
International Journal of Heat and Mass Transfer 48 (2005) 573–583
International Journal of HEAT and MASS TRANSFER
www.elsevier.com/locate/ijhmt

Tree-shaped networks with loops

W. Wechsatol [a], S. Lorente [b], A. Bejan [a,*]

[a] Department of Mechanical Engineering and Materials Science, Duke University, Box 90300, Durham, NC 27708-0300, USA
[b] Laboratory for Materials and Durability of Constructions, National Institute of Applied Sciences (INSA), 135 Avenue de Rangueil, Toulouse 31077, France

Received 19 February 2004; received in revised form 23 August 2004
Available online 11 November 2004

Abstract

Dendritic flow architectures are being contemplated for thermal designs that provide high heat transfer densities for the cooling of electronics. Optimized tree networks maximize the flow access between one point (source, sink) and an infinity of points (line, area, volume). This paper is a fundamental study of a new class of dendritic flow architectures for thermal design: trees combined with closed-loop structures, as in the venation of leaves. The loops provide robustness to the design: the network continues to serve its assigned area even if one or more ducts are damaged. The study documents the achievement of performance and robustness systematically, by starting from the simplest architectures and proceeding toward the more complex, namely, point-circle networks with one loop size and two loop sizes, and networks with loops without and with branching levels. It is shown that the use of loops increases the global flow resistance relative to the dendritic design without loops. Damage, or removal of a duct from the network, also leads to an increase in global flow resistance. These effects become less important as complexity increases, provided that the network is optimized. A damaged peripheral duct induces a smaller penalty than a damaged duct that is situated close to the center of the network. In summary, optimized complex flow structures are robust. Loops are an attractive design feature for maintaining a high level of global performance when the structure experiences local damage.

Keywords: Dendritic networks; Tree-shaped; Constructal; Fractal; Loops; Robustness; Complexity

1. Introduction

Tree networks represent a new trend in the optimization and miniaturization of heat transfer devices [1–4], mass exchangers [5,6], chemical reactors [7], and fuel cells [8]. Tree-shaped architectures promise a more judicious use of the available space: higher densities of heat and mass transfer and chemical reactions, and a more uniform volumetric distribution of transport processes. The fundamental study of the optimization of tree-shaped architectures also sheds light on the common design principles of engineered and natural flow systems.

The tree networks that have been optimized so far are true trees, that is, networks without loops (networks that are not "nets"). The tree makes a unique connection between the root and one point in the canopy (the canopy can be a line, area, or volume). There are as many such connections as there are points in the canopy. If one of these paths is interrupted by accident, then one or more points in the canopy are not served by the network. The design question then is how to protect such points

* Corresponding author. Tel.: +1 919 660 5309; fax: +1 919 660 8963.
E-mail address: dalford@duke.edu (A. Bejan).

0017-9310/$ - see front matter © 2004 Elsevier Ltd. All rights reserved.
doi:10.1016/j.ijheatmasstransfer.2004.08.020

Nomenclature

D	tube diameter, m
L	tube length, m
f	dimensionless flow resistance
$\dot{m}$	mass flow rate, kg m^{-1}
n	number of tubes
N	number of ports on disc perimeter
R	disc radius, m
V	tube volume, m^3
T	temperature, K

Greek Symbols

ΔP	pressure drop, $N\,m^{-2}$
v	kinematic viscosity, $m^2\,s^{-1}$
ρ	fluid density, $kg\,m^{-3}$

Subscripts

i	rank of tube
min	minimum
opt	optimum
0	tube touching the center, Fig. 2
1, 2,...	tube positioned progressively closer to the perimeter
o	disc center
a, b,...	nodal indexes

Superscript

($\hat{}$)	dimensionless, Eqs. (4) and (5)

against the possible loss of direct flow from or to the root.

The solution is put on display in the design of most botanical tree leaves (e.g., Fig. 1a). As in the constructal trees [1], the regions that surround the smallest nerves are served by diffusive flows. The duct flows are concentrated in the nerves, which are organized in tree-like fashion at the larger and more visible scales (e.g., near the root). The smallest nerves, however, are organized additionally into closed loops [9]. With such a structure, the leaf area surrounded by the loop is served by the peripheral duct flow even in cases where the peripheral duct is severed (by a worm, for example). This looped design stands in sharp contrast to the quasi-radial dendritic design of the ginkgo leaf (Fig. 1b), which is the exception—a living fossil the design of which has not changed in millions of years. Speaking of fossils, the tree design with loops at the smallest length scales is a defining feature of the blood vessels used for temperature control in the wings of a pterosaur [10], as reproduced in Fig. 1c.

Tree networks with built-in loops are also employed in man-made systems, for example, in networks for the distribution of electricity and water, and the collection of city waste and rain water. Grids for city traffic can also be superposed tree networks with loops. If in case of accident the flow in one link is interrupted, the flow in neighboring links changes so that the damaged area of the network continues to perform its function.

In this paper we examine the most fundamental attributes of tree networks with loops at smaller scales. In exchange for their increased design resistance (robustness) in case of accidental damage, are they much less efficient than the tree-shaped structures without loops? We examine this issue systematically, optimizing the complete architectures of networks with loops, and comparing their performance with the performance of the correspondingly optimized tree networks without loops. We pursue this study in the direction of increasing complexity, from the simplest tree structure in which only one loop size is present (e.g., Fig. 2b), to structures with two or more loop sizes.

2. Disc-shaped tree canopies

Some of the simplest tree structures are those that connect a point with many points arranged on a line. Such tree structures have been optimized for minimal global flow resistance [11], as well as for minimal flow path lengths [12]. The applications that have stimulated the optimization of trees range from the convection cooling of packages of electronics [2–4] to urban hydraulics problems such as the distribution of hot or cold water to users arranged uniformly on an area [13]. One example is the flow connection between a circle and its center. The users can be approximated by number of discrete outlets arranged equidistantly. Cases with six and three outlets are shown in the examples of Figs. 2a and b, where each network has one level of branching indicated by the dashed circle.

The objective is to minimize the overall pressure drop across a point-circle flow structure such as Fig. 2b. We do this by selecting optimally every geometric feature of the architecture. When the total fluid mass flow rate ($\dot{m}$) from the center to the circle is specified, the minimization of the overall pressure drop (ΔP) is equivalent to minimizing the global flow resistance ($P/\dot{m}$), pumping power ($\dot{m}\Delta P/\rho$), or rate of entropy generation by fluid friction ($\dot{m}\Delta P/\rho T$).

The size of the flow system is represented by two global parameters, or two 'properties' [14]. The external size

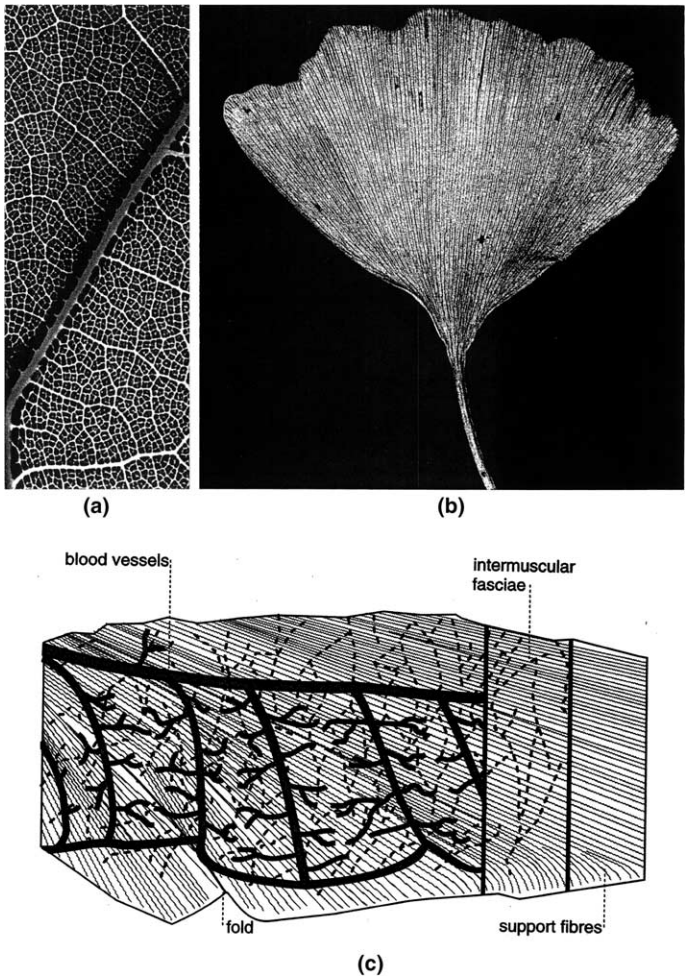

Fig. 1. The design of the nerves of the leaf; (a) The common design, showing tree structure at large length scales, and closed loops at smaller scales; (b) Dendritic design in the ginkgo leaf (*Ginkgo biloba*); (c) tree and loops design in the blood vascularization of the wing of the pterosaur *Rhamphorhynchus muensteri* [10].

is represented by the external length scale R, which is the radius of the circle. The internal size is represented by the volume occupied by all the tubes, V. The geometric variables that account for the morphing of the point-circle flow structure are the number of outlets (N), the number of central tubes (n_0), the number of pairing or bifurcation levels, the duct lengths (e.g., L_0 and L_1 in Fig. 2), and the duct diameters (e.g., the diameters D_0 and D_1 that correspond to the lengths L_0 and L_1 in Fig. 2b). Not all these variables represent degrees of freedom in the design.

3. One loop size

The model selected for the flow through each duct depends on the scale of the flow network. In urban design, for example, the networks for the distribution and collection of water operate in the turbulent regime. At much smaller scales, the cooling networks contemplated for the design of high-density electronics, the flow is laminar, but ducts may be short and the concentrated pressure losses due to entrances and junctions may not be negligible [15–18]. In this section we begin with the simplest model, which consists of straight tubes with round cross-sections, and fully-developed laminar flow in every duct. The L_i/D_i ratio of each tube is assumed to be sufficiently large so that the pressure drop associated with the tube (ΔP_i) is due almost entirely to fluid friction in the straight section L_i. In other words, we neglect the local pressure losses associated with the Y-shaped pairings or bifurcations. This model is chosen for simplicity, and to construct a meaningful basis of comparison with optimized trees without loops [11],

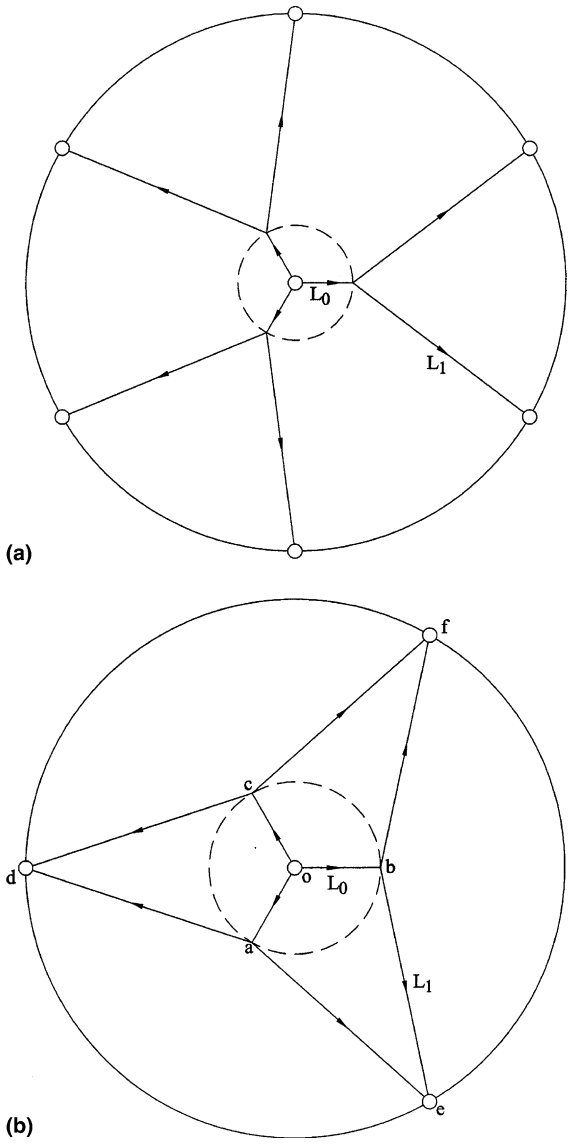

Fig. 2. Arrangement of tubes for flow between the center and a number of points positioned equidistantly on the circle: (a) optimized tree structure with one level of pairing, and (b) the geometric features of a network with loops of one size.

where the same model was used. According to this model, the pressure drop along a tube of length L_i is

$$\Delta P_i = \dot{m}_i \frac{128\nu}{\pi} \frac{L_i}{D_i^4} \tag{1}$$

The radial position of the branching points is indicated with a dashed circle. The calculation of the overall pressure drop $\Delta P = \Delta P_{oe}$ requires the use of Kirchoff's law, according to which we assign one sense (e.g., counterclockwise) to reading each loop. For the loop *oaebo* in Fig. 2b the pressure drops add up to zero, $\Delta P_{oa} + \Delta P_{ae} + \Delta P_{eb} + \Delta P_{bo} = 0$. The minimization of the overall flow resistance $\Delta P/\dot{m}$ requires the use of symmetry: for example, *oe* is the axis of symmetry of figure *oaeb*, and there are only two tube sizes, D_0 ($=D_{oa} = D_{ob} = D_{oc}$) and D_1 ($=D_{ae} = D_{be} = D_{bf} = D_{cf} = D_{cd} = D_{ad}$).

In summary, the geometry of Fig. 2b has only three degrees of freedom (n_0, L_1/L_0, D_1/D_0) when the number of loop sizes (or pairing levels) are fixed. The overall pressure drop ($\Delta P = \Delta P_{oa} + \Delta P_{ae}$) can be expressed as the dimensionless global flow resistance

$$f = \frac{\Delta P}{\dot{m}} \frac{V^2}{8\pi\nu R^3} \tag{2}$$

where

$$f = n_0 \left[\widehat{L}_0 + \frac{1}{2} \left(\frac{D_0}{D_1} \right)^4 \widehat{L}_1 \right] \left[\widehat{L}_0 + 2 \left(\frac{D_1}{D_0} \right)^2 \widehat{L}_1 \right]^2 \tag{3}$$

$$(\widehat{L}_0, \widehat{L}_1) = (L_0, L_1)/R \tag{4}$$

The external and internal constraints (R,V) have been taken into account in the derivation of Eq. (3). Note that when n_0 is fixed, only one of the two lengths $\widehat{L}_0$ and $\widehat{L}_1$ can be varied independently. This degree of freedom accounts for the movable radius of the dashed circle in Fig. 2b. The analysis leading to Eq. (3) is the same as the method presented in Ref. [11] and is not repeated here.

The dimensionless flow resistance f can be minimized with respect to $\widehat{L}_0$ and D_1/D_0. The optimized D_1/D_0 ratio is $2^{-1/3}$, in agreement with Murray's law [1]. The minimal-f results are shown as the "one loop size" curve in

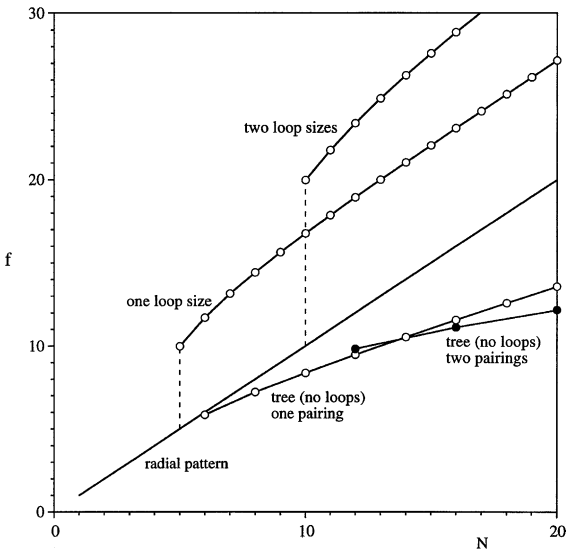

Fig. 3. The minimized global resistance of structures with one and two loop sizes, relative to the global resistance of radial designs and trees without loops.

Fig. 3. The abscissa shows the number of outlets on the rim (N), which in the case of a single loop size is the same as the number of radial tubes (n_0). We found that the one-loop layout can be optimized when $N \geqslant 5$. When N is smaller than 5, the optimal tube arrangement is radial, without loops. The optimized layout of tubes for $N = 5$ is shown in Fig. 4a. As N increases, the central tubes ($\widehat{L}_0$) become longer, as shown for $N = 10$ in Fig. 4b. This behavior is summarized in Fig. 5.

The optimization of the radius of bifurcation ($\widehat{L}_0$) is the same as the optimization of the angle between the two $\widehat{L}_1$ branches that extend beyond the radial duct of length $\widehat{L}_0$. The two $\widehat{L}_1$ ducts and the radial $\widehat{L}_0$ duct form a Y-shaped structure the end points of which are fixed. An earlier study has shown that the angle of the Y configuration can be optimized for minimal global flow resistance [19]. The opportunity to optimize the angle resurfaces here in the optimization of the radial position of the bifurcation.

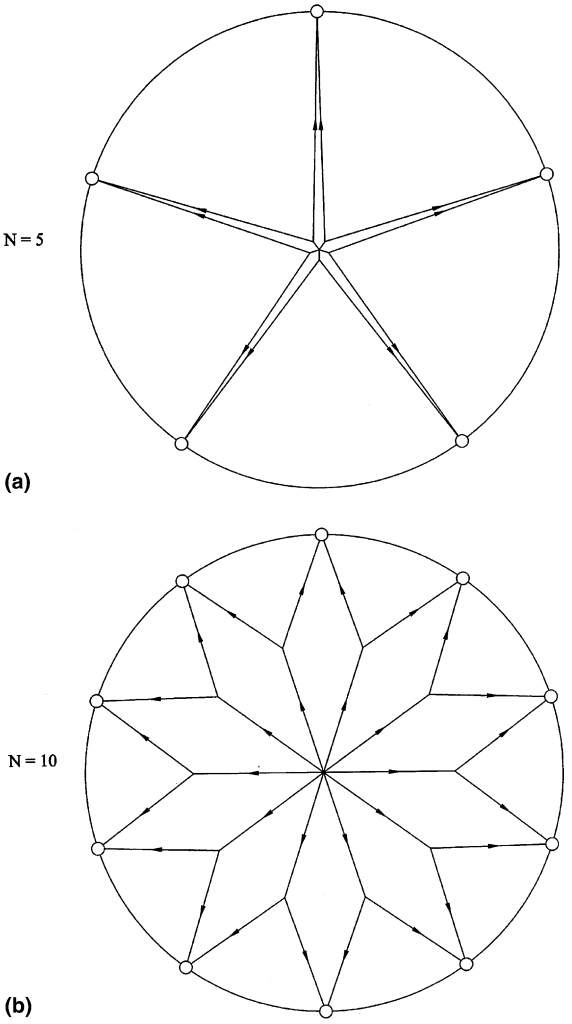

Fig. 4. The optimal layout of tubes with one loop size ($N = 5$, 10).

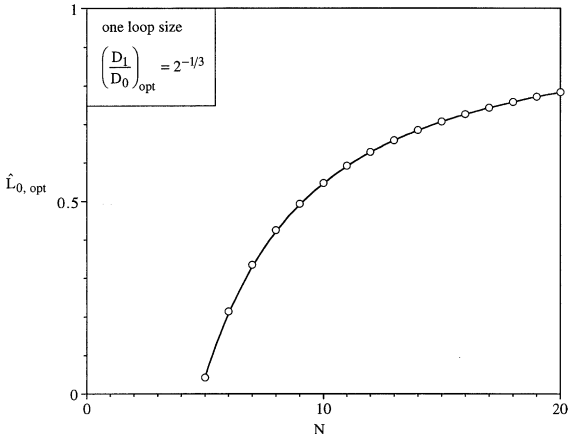

Fig. 5. The optimized central tube length for structures with one loop size.

Fig. 5 confirms that for structures with $N < 5$ an optimal $\widehat{L}_0$ does not exist. The optimization of the one-loop-size structure of Fig. 2b undergoes a transition from $N = 4$ to $N = 5$. Fig. 3 shows that the use of optimized loops causes a significant jump in the global fluid resistance: the f value doubles relative to the design with purely radial tubes. Another manifestation of this type of transition was observed in the optimization of tube layouts without loops: see the lowest curve in Fig. 3, where for $N \geqslant 6$ the lowest f value belongs to trees without loops and one level of pairing. When $N > 14$, the tree with the lowest f values has two levels of pairing.

4. Two loop sizes

Are the structures with loops always inferior to structures without loops? If so, is the inferiority of structures with loops always as severe as we found for the one loop size in Fig. 3? We pursued these questions by looking at increasingly more complex structures with loops and without loops. Fig. 6 shows two optimized structures, each having two loop sizes. There are three generations of tubes (L_i, D_i; $i = 0, 1, 2$), where $i = 0$ indicates the tubes that touch the center, and $i = 2$ the tubes that touch the periphery. The number of ports on the periphery (N) is equal to the number of radial tubes (n_0). The flow model is the same as in the preceding section. The global constraints continue to be the total duct volume (V), the disc radius (R), and the total mass flow rate ($\dot{m}$).

The two-loop configuration has five degrees of freedom: n_0, L_0/R, L_1/R, D_1/D_0 and D_2/D_1. The global flow resistance of the structure is represented by Eq. (5), where the dimensionless resistance f is now given by

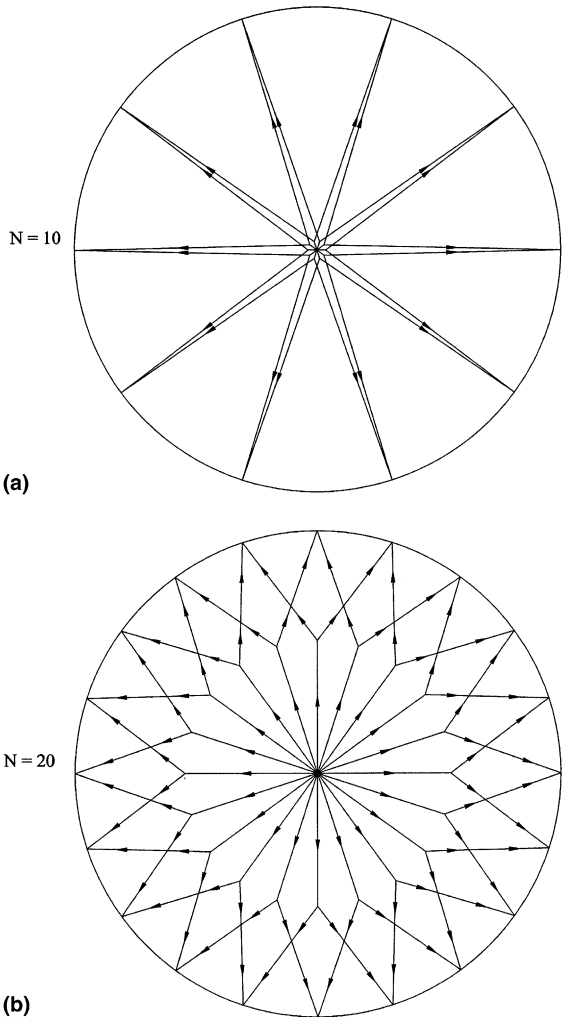

Fig. 6. The optimal layout of tubes with two loop sizes ($N = 10$, 20).

$$f = n_0\left[\widehat{L}_0 + \frac{1}{2}\left(\frac{D_0}{D_1}\right)^4\widehat{L}_1 + \frac{1}{4}\left(\frac{D_0}{D_1}\right)^4\left(\frac{D_1}{D_2}\right)^4\widehat{L}_2\right] \times\left[\widehat{L}_0 + 2\left(\frac{D_1}{D_0}\right)^2\widehat{L}_1 + 4\left(\frac{D_1}{D_0}\right)^2\left(\frac{D_2}{D_1}\right)^2\widehat{L}_2\right]^2 \quad (5)$$

with $(\widehat{L}_0, \widehat{L}_1, \widehat{L}_2) = (L_0, L_1, L_2)/R$. The derivation of Eq. (5) follows the method of Ref. [11]. The minimization of f with respect to the diameter ratios yields $(D_1/D_0)_{\text{opt}} = 2^{-1/3}$ and $(D_2/D_1)_{\text{opt}} = 1$. This means that the loop that touches the rim is composed of tubes of the same size. The optimal two-loop configuration consists of two identical trees with one level of pairing, which are connected to the same N ports on the rim, and which are offset relative to each other by an angle $2\pi/N$. The minimization of f with respect to $\widehat{L}_0$ and $\widehat{L}_1$ was performed numerically, and the results are presented in

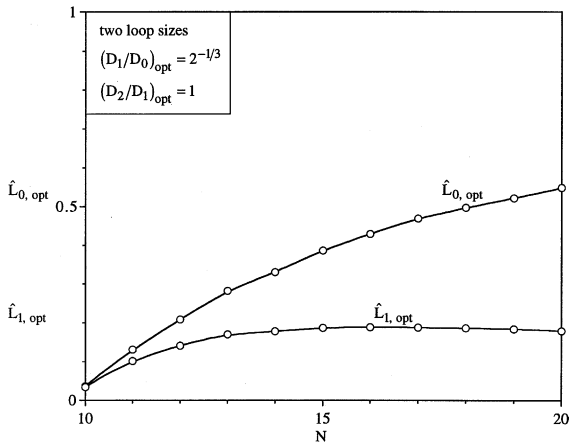

Fig. 7. The optimized tube lengths for structures with two loop sizes.

Fig. 7. Optimized tube lengths were found only for $N \geqslant 10$. The length of the radial tubes increases noticeably as N increases. The length of the intermediate-level tubes $(\widehat{L}_{1,\text{opt}})$ becomes insensitive to changes in N when N is greater than approximately 15. The optimized layouts for $N = 10$ and $N = 20$ have been drawn to scale in Fig. 6.

The minimized overall flow resistance that corresponds to Figs. 6 and 7 is reported as the curve labeled "two loop sizes" in Fig. 3. This curve shows a 'transition' at $N = 10$, below which the optimized flow structures have one loop size, radial tubes, or trees with one level of pairing. When $N = 10$, the f value doubles in size as the structure changes from the radial pattern to the one with two loop sizes. Furthermore, when $N = 10$ the f value increases by a factor of 1.2 if the optimized one-loop configuration is replaced by the optimized two-loop design.

To summarize, the addition of loops to the flow structure causes jumps in the overall flow resistance. This behavior matches what we found in Section 3, where the comparison was between radial tube patterns and designs with only one loop size.

5. One loop size, no branching levels

There is an even simpler class of flows that connect a circle with its center, in such a way that the loops are available on 'stand-by', in case of accidental loss of flow through one radial duct. The main features of this class are shown in Fig. 8. Radial tubes connect the center with N points on the circle. In addition, there are ducts that connect each pair of adjacent points on the circle. Because of symmetry, these peripheral ducts carry no flow, and all the flow between the circle and the center occurs

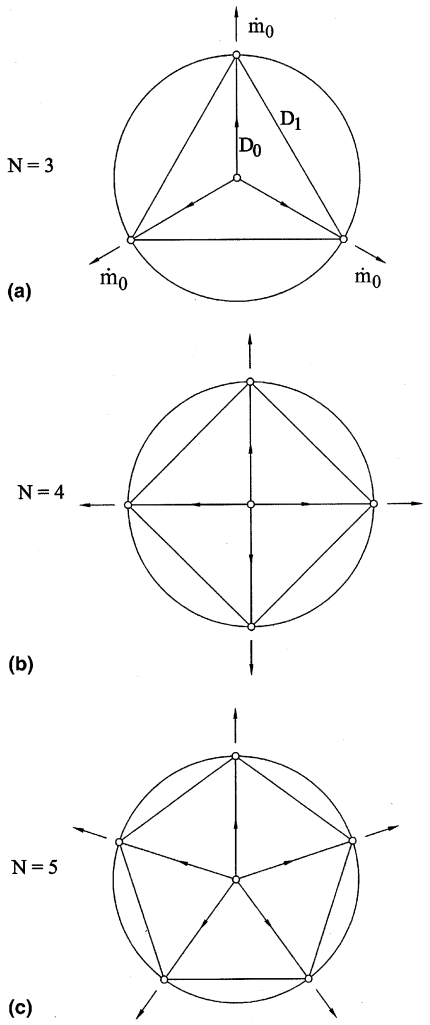

Fig. 8. Structures with one loop size, radial and peripheral tubes, and no branching levels.

through the radial ducts. In this case, the structures of Fig. 8 are represented by the purely radial designs with N radial ducts and N points on the circle, the global performance of which is presented in Fig. 3.

The designs of Fig. 8 are interesting and useful for another reason, which calls for the existence of loops. If one of the radial tubes is cut off, then the N points on the circle continue to be served by the flow network. This 'survival' capability is not offered by the radial flow patterns.

Consider the simplest member of the class of Fig. 8, namely the case $N = 3$. The three peripheral points continue to be connected under two accident scenarios: loss of flow through one radial tube, and loss of flow through two radial tubes. The design lessons taught by this class are new relative to what we learned so far from networks with loops. They are about the continuation of performance in the wake of the loss of one or more ducts. For the structure with $N = 3$, there are three levels of performance, in descending order:

(i) No interruption of flow through the radial tubes.
(ii) One radial tube is cut off. The peripheral tubes that make up for the damaged tube must have their diameters sized optimally, so that under this scenario the performance is the highest that it can be. All the peripheral tubes must have the same diameter, because it is not known a priori which radial tube stops functioning.
(iii) Two radial tubes are cut off. Here we have the same questions and optimization opportunities as at (ii), but we expect a global performance that is inferior relative to both (ii) and (i).

Consider case (i) where none of the radial tubes are interrupted, Fig. 8a. Ducts with arrows indicate flow. Ducts without arrows have no flow, because of symmetry. There are only two tube sizes, D_0 and D_1. Because the total tube volume is fixed, the smallest global resistance f is attained when all the tube volume is allocated to the tubes with flow: this base design with only radial tubes is represented by the point shown for $N = 3$ on line C in Fig. 10.

When one radial tube is cut off, Fig. 9a, the flow rates adjust themselves so that each of the three peripheral points receives the required flow rate $\dot{m}_0$. The dimensionless global resistance for this configuration is (in accordance with the method of Ref. [11])

$$f = 3\left[\frac{3}{2} + \sin\left(\frac{\pi}{3}\right)\left(\frac{D_0}{D_1}\right)^4\right]\left[1 + 2\sin\left(\frac{\pi}{3}\right)\left(\frac{D_1}{D_0}\right)^2\right]^2 \quad (6)$$

where f continues to be defined as in Eq. (2). This function reaches its minimum ($f = 47.98$) when $D_1/D_0 = 0.833$. The performance of this design is indicated at $N = 3$ on curve A in Fig. 10.

What if the D_1/D_0 ratio is optimized for operations with one interrupted radial tube (Fig. 9a), but all the radial tubes function? In this case, the peripheral tubes have finite-size diameters even though they carry no flow. The global flow resistance for $N = 3$ is $f = 14.54$, which falls between the f values calculated for Fig. 9a and the limit where the peripheral tubes are absent. This intermediate design is represented by the middle curve in Fig. 10: an undamaged network with loops on standby, which is designed for optimal operation when damaged.

The three designs illustrated above for $N = 3$ have been determined for many other networks with one loop size and no branching levels. The results are summarized as curves A, B and C in Fig. 10. The performance of designs with loops (A, B) is inferior to that of designs without loops (C). In relative terms, however, all designs

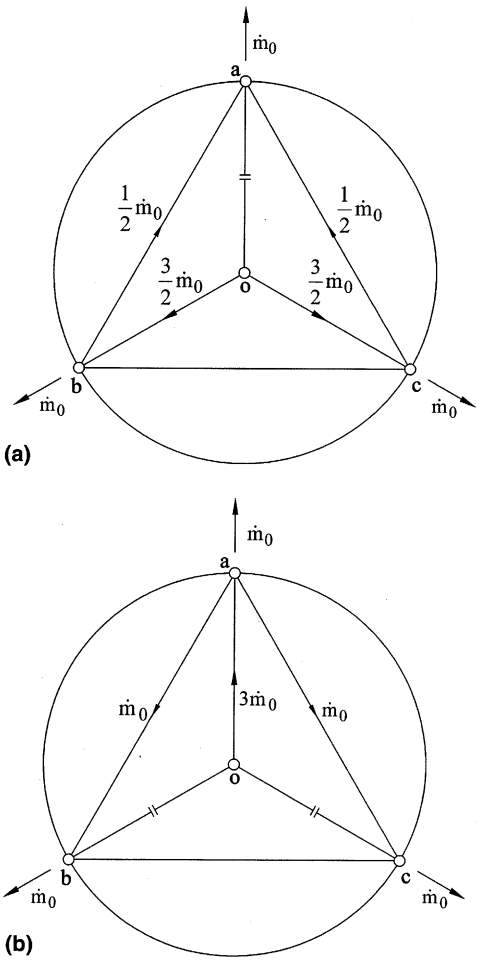

Fig. 9. The case of Fig. 8a with one and two radial tubes cut off.

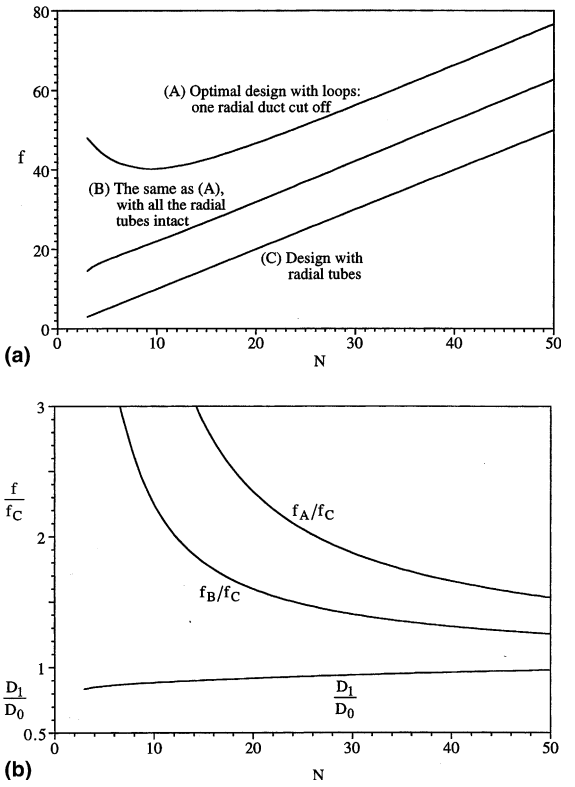

Fig. 10. The robustness of optimized complex flow structures: loops (A, B) vs. no loops (C), and damage (A) vs. no damage (B, C).

operate at comparable levels as the complexity (N) increases.

The lower graph of Fig. 10 illustrates the robustness of optimized complex flow structures. Although damage (f_A, f_B) decreases performance, the impact of cutting off one tube is relatively small when the network is complex. Furthermore, to have loops on standby (undamaged) means to pay a penalty relative to no loops at all ($f_B > f_C$). When the network is complex this penalty becomes minor—it becomes a good investment in the survival of the flow structure under damage.

The D_1/D_0 curve in the lower graph of Fig. 10 shows the optimized ratio of diameters when only one tube is cut. This ratio is relatively insensitive to changes in complexity. When N becomes large, the loop becomes uniform: the diameter of the peripheral tubes approaches that of the radial tubes.

The more complex the flow structure, the more numerous the ducts that can be damaged. The first opportunity to explore this direction is offered by the structure of Fig. 9b, where two radial tubes are cut off. Optimization shows that in this case the optimal ratio of diameters is the same as in Fig. 9a, namely $D_1/D_0 = 0.833$, and that the minimized f value is exactly twice the f value of Fig. 9a, namely $f = 47.98$. Greater damage means decreased performance.

Fig. 11 shows the two ways in which two tubes can be cut off in the $N = 4$ structure of Fig. 8. The optimized designs are reported in Table 1 along with the designs with one and three cut tubes. The table also shows the design optimized to operate with one missing tube, but when the tube is present. Once again, the greater the damage the lower the performance level.

Another interesting aspect is the great difference between the performance of the designs of Fig. 11a and Fig. 11b. Both designs have two tubes missing. Performance is superior when one damaged tube acts as counterweight to the other (Fig. 11a). We may say that a relatively high level of performance is maintained when the damage is distributed more uniformly through the structure. This conclusion is qualitatively the same as the 'optimal distribution of imperfection' principle of constructal design, where the flow resistances are distrib-

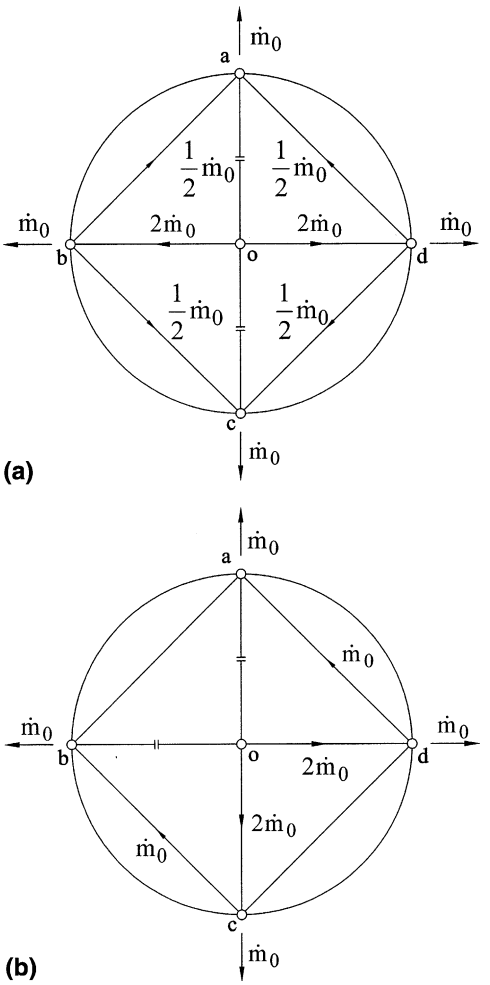

Fig. 11. The case of Fig. 8b with two radial tubes cut off.

Table 1
Optimized networks with $N = 4$, one loop size, and no branching levels (Fig. 8b)

Radial tubes missing	f_{min}	$(D_1/D_0)_{opt}$
0	16.35	0.85
1	45.24	0.85
2 (Fig. 11a)	54.09	0.794
2 (Fig. 11b)	76.49	0.891
3	152.98	0.891

uted in space such that the global performance is maximized.

6. One loop size, one branching level

The design of loops into more complex structures reinforces the conclusions of the preceding section. Consider first the tree-shaped network shown in Fig. 12a: four central tubes, eight peripheral ports, and one branching level. Loopless architectures of this type have been optimized in [11], which showed that the optimal design in Fig. 12a is characterized by the tube lengths $L_0 = 0.425R$ and $L_1 = 0.629R$. The optimal D_1/D_0 and f values are listed in the top row of Table 2.

Loops of one size are created by connecting each pair of adjacent peripheral ports, as shown in Fig. 12b. There are three tube sizes, and the allocation of tube volume is characterized by the ratios D_1/D_0 and D_2/D_1. When none of the tubes is missing, symmetry dictates zero flow through the peripheral tubes. The latter are present because they are needed in case one or more of the inner tubes is cut off.

Figs. 13a and b show the two ways in which one of the inner tubes is removed. The f values for these two cases are listed in Table 2: it is relatively unimportant which tube is cut off, the one that reaches the center, or the one that reaches the periphery. A slight advantage

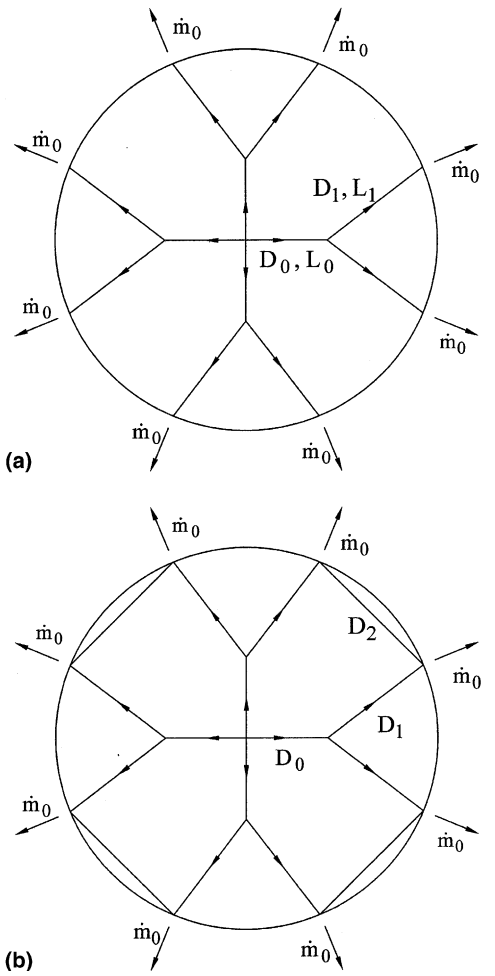

Fig. 12. Network with four central tubes and one level of branching: (a) no loops; (b) one loop size.

Table 2
Optimized networks with one loop size and one branching level (Figs. 12 and 13)

Tubes missing	f_{min}	$(D_1/D_0)_{opt}$	$(D_2/D_1)_{opt}$
0 (no loops, Fig. 12a)	7.213	$2^{-1/3}$	
0 (Figs. 13a,b, uncut)	14.35	$2^{-1/3}$	1.018
1 (Fig. 13a)	36.59	$2^{-1/3}$	1.018
1 (Fig. 13b)	36.61	$2^{-1/3}$	1.018

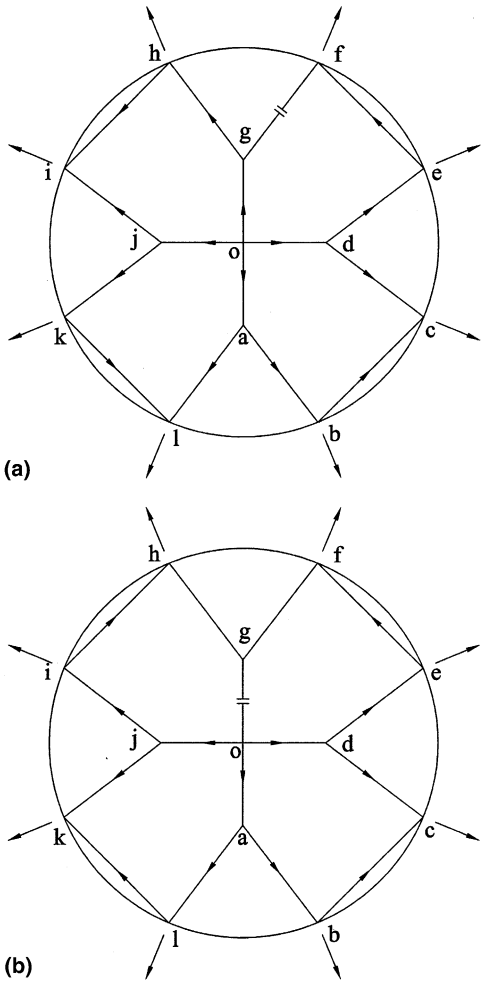

Fig. 13. Two ways to cut one tube from the design of Fig. 12b.

goes to the design of Fig. 13a, suggesting that damage has lesser impact when it occurs near the periphery, in the tree canopy, not near the trunk.

Table 2 also shows the performance of the designs of Figs. 13a and b when all the tubes are intact (as in Fig. 12b). Overall, the message of the one-loop-size networks summarized in Table 2 is similar to that of Table 1. Optimized complex structures are robust. Loops are

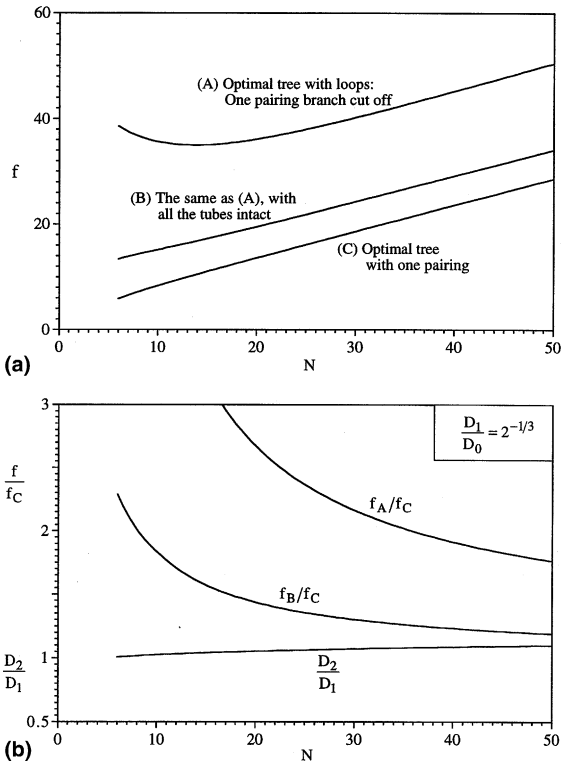

Fig. 14. The effect of tube damage on the performance of designs with one loop size and one branching level.

needed in order to maintain global performance when the structure experiences local damage.

The optimization of architectures with one loop size and one branching level, which in Figs. 12 and 13 was illustrated for $N = 8$, was repeated for many other cases of this type. The results are summarized in Fig. 14. Because there is little difference in the flow resistance (f) between cutting one peripheral branch (Fig. 13a) and cutting a central duct (Fig. 13b), in the upper frame of Fig. 14 (curve A) we plotted only the f values resulting when one peripheral branch is cut off. The lower frame of Fig. 14 reports the optimal tube size ratio D_2/D_1, which is close to 1. Fig. 14 also shows that the relative performance ratios f_A/f_C and f_B/f_C decrease toward 1 as N increases, indicating robustness as complexity increases. Fig. 14 is qualitatively the same as Fig. 10. The effect of tube damage loses its impact, and can be tolerated when the network is not only complex but also optimized.

7. Concluding remarks

In this paper we examined the effect of using loops in tree-shaped networks for distribution and collection of

fluid over an area. Networks with loops and without loops were optimized and compared on the same basis: the same overall size of the spanned territory, and the same total duct volume.

Networks with loops offer a great advantage: in case of accidental damage in one of the links of smallest scales the surviving arc of the loop assures the continuity of flow to and from the elemental area covered by the loop. Because of this feature, the network continues its function, and, in spite of the damage, the network registers only a small drop in global performance (Fig. 10).

The disadvantage of trees with loops is that in the absence of accidental damage their performance is inferior to that of trees without loops. This feature was documented in several cases with increasing complexity (Figs. 2–6).

A general observation concerning Fig. 3 is that each curve represents the 'envelope' above which lies the 'cloud' of larger f values of the infinite number of non-optimal designs (non-equilibrium configurations) that have the same types and numbers of geometric features [14]. For example, the "two loop sizes" curve is the bottom lining of the cloud filled by the (f, N) points representing the non-optimal structures with two loop sizes.

The current progress on tree-shaped flow architectures and their technological applications is reviewed in two new books [20,21]. In particular, the minimization of flow resistance does not always lead to the same architecture as the minimization of pumping power, as shown in Ref. [22].

Acknowledgments

This work was supported by the National Science Foundation. Mr. Wechsatol acknowledges the support received from the Royal Thai Government and King Mongkut's University of Technology (KMUTT), Thailand.

References

[1] A. Bejan, Shape and Structure, from Engineering to Nature, Cambridge University Press, Cambridge, UK, 2000.
[2] Y. Chen, P. Cheng, Heat transfer and pressure drop in fractal tree-like microchannel nets, Int. J. Heat Mass Transfer 45 (2002) 2643–2648.
[3] D.V. Pence, Reduced pumping power and wall temperature in microchannel heat sinks with fractal-like branching channel networks, Microscale Thermophys. Eng. 6 (2002) 319–330.
[4] Z.Z. Xia, Z.-X. Li, Z.-Y. Guo, Heat conduction optimization: high conductivity constructs based on the principle of biological evolution, In: Twelfth Int. Heat Transfer Conf., Grenoble, France, 18–23 August 2002.
[5] D. Tondeur, L. Luo, U. d'Ortona, Optimisation des transferts et des matériaux par l'approche constructale, Entropie 30 (2000) 32–37.
[6] A. Rivera-Alvarez, A. Bejan, Constructal geometry and operation of adsorption processes, Int. J. Thermal Sci. 42 (2003) 983–994.
[7] M.-O. Coppens, Y. Cheng, C.M. van den Bleek, Controlling fluidized bed operation using a novel hierarchical gas injection system, Paper 304d, AIChE Annual Meeting, Dallas, TX, October 31–November 5, 1999.
[8] J.V.C. Vargas, A. Bejan, Thermodynamic optimization of internal structure in a fuel cell, Int. J. Energy Res. 28 (2004) 319–339.
[9] E.P. Klucking, Leaf Venation Patterns: The Classification of Leaf Venation Patterns, vol. 7, J. Cramer, Berlin, 1995.
[10] E. Frey, H. Tischlinger, M.-C. Buchy, D.M. Martill, New specimens of Pterosauria (Reptilia) with soft parts with implications for pterosaurian anatomy and locomotion, in: E. Buffetaut, J.-M. Mazin (Eds.), Evolution and Palaeobiology of Pterosaurs, Special Publications, vol. 217, Geological Society, London, 2003, pp. 233–266.
[11] W. Wechsatol, S. Lorente, A. Bejan, Optimal tree-shaped networks for fluid flow in a disc-shaped body, Int. J. Heat Mass Transfer 45 (2002) 4911–4924.
[12] S. Lorente, W. Wechsatol, A. Bejan, Tree-shaped flow structures designed by minimizing path lengths, Int. J. Heat Mass Transfer 45 (2002) 3299–3312.
[13] W. Wechsatol, S. Lorente, A. Bejan, Tree-shaped insulated designs for the uniform distribution of hot water over an area, Int. J. Heat Mass Transfer 44 (2001) 3111–3123.
[14] A. Bejan, S. Lorente, The constructal law and the thermodynamics of flow systems with configuration, Int. J. Heat Mass Transfer 47 (2004) 3203–3214.
[15] J. Padet, Fluides en Écoulement, Masson, Paris, 1991.
[16] A. Lallemand, Écoulement des Fluides, Techniques de l'Ingénieur—Traité de Génie Energétique, vol. BE, Article 8161, 2001.
[17] I.E. Idelchik, Handbook of Hydraulic Resistance, second ed., Hemisphere, Washington, DC, 1986.
[18] A. Boussicaud, Calcul des pertes de charge, Editions Parisiennes, Paris, 1990.
[19] A. Bejan, L.A.O. Rocha, S. Lorente, Thermodynamic optimization of geometry: T- and Y-shaped constructs of fluid streams, Int. J. Thermal Sci. 39 (2000) 949–960.
[20] A. Bejan, I. Dincer, S. Lorente, A.F. Miguel, A.H. Reis, Porous and Complex Flow Structures in Modern Technologies, Springer-Verlag, New York, 2004.
[21] R.N. Rosa, A.H. Reis, A.F. Miguel (Eds.), Bejan's Constructal Theory of Shape and Structure, Évora Geophysics Center, University of Évora, Portugal, 2004.
[22] L. Gosselin, A. Bejan, Tree network for minimal pumping power, Int. J. Thermal Sci. 44 (2005) 53–63.